Energy Efficient Arrival with RTA Constraint for Urban eVTOL Operations

Priyank Pradeep * Peng Wei †

The electric vertical takeoff and landing (eVTOL) air taxis can alleviate transportation congestion on the ground by utilizing three-dimensional airspace efficiently. However, the endurance of Lithium-ion Polymer (Li-Po) batteries imposes severe constraints on the operational time span of an eVTOL vehicle on an urban air mobility (UAM) passenger transport mission. This research focuses on the formulation of fixed final time multiphase optimal control problem with energy consumption as the performance index for a multirotor eVTOL vehicle. The proposed multiphase optimal control problem formulation and the numerical solution enables the eVTOL air taxi to meet the given required time of arrival (RTA) and achieve the most energy efficient arrival trajectory, which is a critical enabler for the safe and efficient future eVTOL operations for passenger transportation and cargo delivery. The problem formulation is validated in a UAM passenger transport use case with EHang 184 eVTOL air taxi and an Uber proposed vertiport in numerical simulations. However, this proposed framework can also be used to address an energy efficient cargo delivery case in a UAS traffic management (UTM) context.

Nomenclature

A	Rotor disk area
D	Drag force
F_x	Equivalent front plate area of the fuselage of the eVTOL air taxi
F_h	Equivalent top plate area of the fuselage of the eVTOL air taxi
h	Altitude of the vehicle
J	Optimal control performance index
m	Mass of the vehicle
P	Power
R	Radius of the rotor
T	Thrust force
v_h	Rotor induced velocity in hover
$(v_h)_e$	Co-axial rotor system effective induced velocity in hover
v_i	Rotor induced velocity during forward flight
V	True airspeed of the eVTOL air taxi
V_x	Component of true airspeed along track
V_h	Component of true airspeed along vertical direction
x	Along track distance of the vehicle from the destination
α	Angle of attack of air-stream relative to rotor tip path plane
γ	Aerodynamic flight path angle
η	Aerodynamic efficiency factor
θ	Rotor tip-path-plane pitch angle
ρ	Density of the air
ω_i	Angular velocity of the i^{th} rotor

*Ph.D. Student, Aerospace Engineering Department, Iowa State University, Ames, IA, 50011
†Assistant Professor, Aerospace Engineering Department, Iowa State University, Ames, IA, 50011

I. Introduction

Every day, millions of man hours are spent unproductively in cities across the world due to road-traffic congestion. In 2014, the congestion caused 3.1 billion gallons of extra fuel burn in the US. Transportation as a whole accounted for approximately 33 % of CO_2 emissions in the US, of which 80 % are from cars and trucks traveling on roadway system.[1] A study in the American Journal of Preventative Medicine, for example, found that those who commute more than 10 miles were at increased odds of elevated blood pressure.[2] The air taxis can alleviate transportation congestion on the ground by utilizing three-dimensional airspace efficiently, just as skyscrapers allowed cities to use limited land more efficiently. A network of small, electric aircraft that take off and land vertically (eVTOL), can enable rapid and reliable transportation between suburbs and cities and, ultimately, within cities.[3] The eVTOLs, can travel toward their destination on a geodesic path, making route-based congestion less prevalent. Over a dozen companies, with many different design approaches, are passionately working to make eVTOLs a reality. The eVTOLs have zero operational emissions as they use electric propulsion.[3–5]

In this paper, we present a framework to perform energy efficient arrival for a multirotor urban eVTOL operations given the required time of arrival (RTA) constraint. With the proposed multiphase optimal control problem formulation and the numerical solution, we enable the eVTOL air taxi to meet the given RTA and achieve the most energy efficient arrival trajectory, which is a critical enabler for the safe and efficient future eVTOL operations for passenger transportation and cargo delivery. Our problem formulation is validated in an urban air mobility (UAM) passenger transport use case with EHang 184 eVTOL air taxi and an Uber proposed vertiport in numerical simulations. However, this proposed framework can also be used to address an energy efficient cargo delivery case in an unmanned aircraft systems (UAS) traffic management (UTM) context.

II. Background and Motivation

A. Background

Since 2013, NASA[4] and its collaborators from government, industry, and academia have contributed to the research and development of UAS traffic management (UTM). They have been focused on small UAS operations, which include cargo delivery proposed by Amazon and Google. However, from 2016 onwards the possibility of urban air mobility (UAM) has also been explored by NASA, Uber, Airbus and university researchers.[3–6]

Most of the UTM and UAM operations of the eVTOL air taxis are under limited battery endurance and vertiport capacity. A few groups such as in Georgia Tech, Purdue University, NASA Ames, and Polytechnic University of Catalonia have worked on commercial jetliners continuous descent operations for energy efficient arrival.[7–14] However, according to our knowledge, no significant research work has been carried out for the energy efficient arrival under time constrained environment for the eVTOL air taxis in the UTM or UAM context. This paper aims to fill this gap to enable safe and efficient eVTOL operations given limited vertiport capacity and eVTOL battery endurance.

B. Motivation

Though electric propulsion is the preferred propulsion choice for the VTOL air taxi, the specific energy (the amount of energy per unit weight provided by the battery) of Lithium-ion polymer (LiPo) batteries today is insufficient for long-range commutes.[3] Also, from the certification point of view eVTOL aircraft may require landing with reserve battery charge/usage time (analogous to reserve fuel in the aircraft).

The research effort on UAS traffic management (UTM) and urban air mobility (UAM), need to address the following two critical operational challenges for cargo delivery and passenger transportation by the eVTOL air taxis:

(i) Generate the optimal energy efficient arrival trajectory given limited battery endurance.

(ii) Satisfy the RTA constraint given the safe aircraft separation and limited vertiport arrival time slots.

Therefore, optimal (minimum battery usage) trajectory generation with RTA constraint is one of the key elements for the operational success of the eVTOL air taxis.

III. Problem Formulation

A. Vehicle Model

The eVTOL air taxi is modeled based on specifications of EHang 184.[15]The vehicle has four arms (4X-configuration) with each arm consisting of two identical coaxial counter-rotating rotors. The rotor tip-path-plane is assumed to be parallel to the horizontal plane of the vehicle.

Figure 1. EHang 184: coaxial multi-rotor eVTOL air taxi with X8-configuration[15]

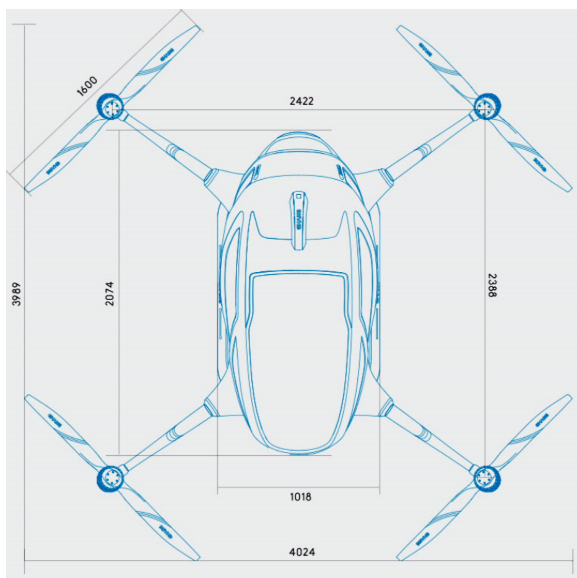

Figure 2. Top view of EHang 184, all dimensions in mm[15]

B. Trajectory Optimization

The lateral path between the initial position of the eVTOL in-air (cruise phase) and the vertiport is assumed to be a geodesic path. Therefore, only the vertical trajectory of the eVTOL air taxi is free for the optimization. However, since the arrival time constraint has been imposed on the eVTOL vehicle, the problem involves generation of an energy-optimal vertical path for the eVTOL vehicle under arrival time constraint.

C. Flight Dynamics Model

In quadrotors roll, pitch and yaw angles are controlled by using various differential thrust mechanism across the rotors. For example, differential thrust between opposite motors provides roll and pitch moments.[16] Previously, researchers[17–19] have successfully decoupled longitudinal and lateral dynamics for helicopters with the conventional design. In general, quadrotors have a more symmetrical design (the location of rotors and the axis of rotation w.r.t center of gravity) than the conventional helicopters. Hence, to simplify the optimal control problem and reduce the computational time, the longitudinal dynamics of the eVTOL air taxi has been decoupled from lateral dynamics.[17–19] This allows us to solve the vertical trajectory generation problem as 2D flight dynamics problem in the vertical plane.

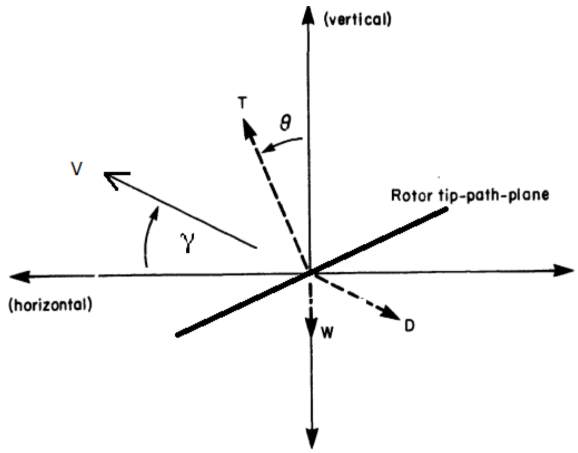

Figure 3. Definition of the vehicle's position, velocity and forces[19]

The two-dimensional longitudinal dynamics model of the vehicle in a fixed inertial frame of reference is as follows:

$$\frac{dV_x}{dt} = \frac{T\sin\theta - D\cos\gamma}{m} \tag{1}$$

$$\frac{dV_h}{dt} = \frac{T\cos\theta - D\sin\gamma - mg}{m} \tag{2}$$

$$\frac{dx}{dt} = V_x \tag{3}$$

$$\frac{dh}{dt} = V_h \tag{4}$$

$$T = T_1 + T_2 + T_3 + T_4 \tag{5}$$

where [x,h] is the position vector (along track distance, altitude) of the center of mass relative to the origin (inertial frame of reference), θ is the rotor tip-path-plane pitch angle, T is the net thrust, D is the net drag, T_i is the net thrust produced by the i^{th} arm (two counter-rotating coaxial rotors), m is the mass, $[V_x,V_h]$ are the horizontal and vertical components of the true airspeed and g is the acceleration due to gravity. Also, the rotor tip-path-plane pitch angle (θ), the rotor angle of attack (α) and the eVTOL vehicle's flight path angle (γ) are related as following:

$$\alpha = \theta + \gamma \tag{6}$$

D. Momentum Theory in Hover

Using momentum theory,[16,20,21] the induced velocity (v_h) in hover is given by:

$$v_h = \sqrt{\frac{T_{rotor}}{2\rho A}} \tag{7}$$

where T_{rotor} is the thrust produced by the rotor, A is the rotor disk area (πR^2), R is the radius of the rotor and ρ is the density of the air.

E. Momentum Theory in Forward Flight

Consider a rotorcraft in forward motion at true airspeed V, with angle of attack α between the air-stream and the rotor disk (tip path plane). The solution for induced velocity (v_i) is:[16,20,21]

$$v_i = \frac{v_h^2}{\sqrt{(V\cos\alpha)^2 + (V\sin\alpha + v_i)^2}} \tag{8}$$

The thrust produced by the ideal rotor per power input:[16,20,21]

$$T_{rotor} = \frac{P_{rotor}}{V\sin\alpha + v_i} \tag{9}$$

F. Coaxial Rotor Interference in Forward Flight

The eVTOL air taxi under consideration has 4 arms, with each arm consisting of two identical counter-rotating rotors. Assuming equal thrust produced by the lower and upper rotors of the coaxial rotor system, the net thrust produced by the arm is given by:

$$T_{arm} = T_{lower} + T_{upper} = 2T_{rotor} \tag{10}$$

Wing theory for a single lifting surface shows that the induced power loss of the arm i.e. coaxial counter-rotating system is:[21]

$$P_{arm} = 2P_{induced}(1+\chi) \tag{11}$$

where $P_{induced}$ is the induced power of an isolated rotor and χ is the rotor interference factor for the coaxial rotor system. Typically, χ is ≤ 1. However, in the current research the interference factor (χ) for all the rotors is assumed to be 1.0.[21]

G. Drag Model

Based on the maximum ground speed of the vehicle (100 km/hr), the vehicle operates in $M < 0.3$ flow regime and hence the drag force on the fuselage of the eVTOL air taxi can be modeled based on the incompressible flow theory. The net drag on the vehicle is assumed to be equivalent to the drag on the fuselage of the vehicle. Therefore, the net drag on the vehicle is calculated as follows:[18,22]

$$D = \frac{\rho V^2 C_D F}{2} \tag{12}$$

where F is the equivalent flat plate area of the fuselage and $C_D = 1$.[18] The horizontal and vertical components of the drag in fixed inertial frame of reference are as follows:

$$D_x = \frac{\rho V_x^2 C_D F_x}{2} \tag{13}$$

$$D_h = \frac{\rho V_h^2 C_D F_h}{2} \tag{14}$$

where F_x and F_h are the equivalent front and top flat plate area of the fuselage respectively.

H. Power Required by the eVTOL Vehicle

Energy balance equation for a multirotor eVTOL vehicle is given by:[18,23]

$$\sum_{i=1}^{N} I_i \omega_i \frac{d\omega_i}{dt} = \sum_{i=1}^{N} P_i - P_{\text{required}} \tag{15}$$

where P_i is the energy supplied to the i^{th} rotor, P_{required} is the instantaneous power required by the vehicle (to overcome induced drag, profile drag, parasite drag and/or gravity to climb), ω_i is the rotational speed of the i^{th} rotor and I_i is the rotational moment of inertia of the i^{th} rotor. However, based on assumption of quasi-steady flight in the current research, the instantaneous power required in forward flight is equal to the sum of the induced power, parasite power, climb power and profile power.[20,21,24]

$$P_{required} = P_{induced} + P_{parasite} + P_{climb} + P_{profile} \tag{16}$$

The profile power exhibits only a slight increase in value with forward speed unless the tip of the rotor is above the critical Mach number.[21] Since the eVTOL vehicle considered in this research is a low speed vehicle with a small rotor diameter (1.6 m), the profile drag is assumed to be constant in magnitude and hence has a negligible impact on the variation of the instantaneous power required. Therefore, in the current research $P_{required}$ is assumed to be:[21]

$$P_{required} = P_{induced} + P_{parasite} + P_{climb} \tag{17}$$

$$P_{required} = 4P_{arm} + TV \sin\alpha \tag{18}$$

where P_{arm} is the induced power loss per arm i.e. coaxial rotors and the term $TV sin\alpha$ is the power required to climb and to propel the eVTOL vehicle forward (the parasite power loss).[21]

I. Performance Index of Multiphase Optimal Control

The power supplied by the battery to the ideal i^{th} motor at time t is given by:[16]

$$P_i(t) = V_i(t)I_i(t) \tag{19}$$

where $V_i(t)$ and $I_i(t)$ is the instantaneous voltage and current across the motor respectively.[16,25] Therefore, by equating the total energy supplied by the battery (or pack of batteries) to the ideal power consumed by all the motors (8 in total), the power consumed by the motors is given by:

$$P(t) = \sum_{i=1}^{8} V_i(t)I_i(t) \tag{20}$$

Hence from the above equation, we can see that in order to minimize battery usage the following performance index needs to be minimized (the Lagrange type problem):

$$J = \int_0^{t_f} \sum_{i=1}^{8} V_i(t)I_i(t)dt \tag{21}$$

The performance index of multiphase optimal control problem for the vertical trajectory optimization of the eVTOL vehicle is as follows:

$$J = \sum_{N=1}^{2} \int_{t_0^N}^{t_f^N} \sum_{i=1}^{8} V_i(t)I_i(t)dt \tag{22}$$

where N is the vertical flight phase (N = 1 for cruise and N = 2 for descent(arrival)).

Assuming that the power supplied by the battery pack is equal to the power required (induced and parasite), ignoring the profile power, the performance index for the vertical trajectory optimization of the eVTOL vehicle is:

$$J = \sum_{N=1}^{2} \int_{t_0^N}^{t_f^N} (\sum_{Arm=1}^{4} P_{arm}(t) + TV \sin\alpha)dt \tag{23}$$

J. Bounds on State and Control Variables

The eVTOL air taxi's pitch angle is assumed to be bounded to 6° for passenger comfortness based on discussions with NASA researchers and experienced helicopter pilots.

$$-6^\circ \leq \theta_{fuselage} \leq 6^\circ \tag{24}$$

The maximum speed (m/s), maximum cruise altitude (m) and total power (KW) is bounded based on specifications of EHang 184[15]

$$0 \leq V_x \leq 27.778 \tag{25}$$

$$0 \leq h \leq 3500 \tag{26}$$

$$P \leq 152 \tag{27}$$

The cruise phase transitions to descent phase at Top of Descent (TOD) waypoint. Hence, TOD i.e. phase transition waypoint is subject to phase link constraints on state variables (X) apart from path and control constraints[26,27] :

$$X^{N-1}(t_f^{N-1}) = X^N(t_0^N) \tag{28}$$

In our initial effort, airspace restrictions on the speed and altitude of the vehicle have been ignored. However, our framework allows us to easily modify bounds on the state and control variables based on new research findings about passenger comfort ability and operational requirements.

K. Avoidance of Vortex Ring State in Descent

When a multi-rotor vehicle starts to descend from the cruise phase, the flow starts to develop recirculation near the disk and turbulence above it.[21,28] However, at small rates of descent, the flow in the vicinity of the disk is still reasonably well represented by the momentum theory model.

In vortex ring state, the flow near the rotor disk becomes highly unsteady and turbulent. Hence, the rotor in this state experiences a very high vibration level and loss of control. In order, to avoid the eVTOL vehicle entering into vortex ring state, the following constraint has been imposed to the descent phase of the problem:[21,28]

$$-0.28 \leq \frac{V \sin\alpha}{(v_h)_e} \leq 0 \tag{29}$$

$$(v_h)_e = \sqrt{\frac{2T_{rotor}}{2\rho A}} \tag{30}$$

where V is the true airspeed of the eVTOL vehicle, T_{rotor} is the thrust produced by the upper/lower rotor of the co-axial rotor system, $(v_h)_e$ is the effective induced velocity in hover of the co-axial rotor system and α is the angle of attack of the tip path plane of the rotors.

L. Required Time of Arrival

Studies and operational trials have been undertaken to investigate the performance and behavior of Required Time of Arrival (RTA) function for the fixed-wing aircraft. RTA enables speed control of the aircraft to meet a Controlled Time of Arrival imposed by Air Traffic Control (ATC).[29] We anticipate implementation of RTA in the trajectory optimization (4D) of eVTOL air taxis would be critical to the traffic management of air taxis in future. In the current research, RTA is imposed as final time constraint on the eVTOL vehicle (EHang 184). Hence, the vertical trajectory optimization problem involves fixed t_f and position $[x_f,\ h_f]$.

$$t_f = RTA \tag{31}$$

M. Autorotation in Descent

The power-off descent of a rotorcraft is called autorotation. The climb/cruise longitudinal flight dynamics model cannot be exactly used for autorotative descent. As in power-off descent, the airstream velocity is directed upward and therefore the far downstream wake is above the rotor disk.[21] For forward descent in power-off state, $|\frac{V \sin\alpha}{V_h}| > 2$ safely avoids power settling for any glide slope angle:[16,20,21] Typically, classical momentum theory can also be applied to forward descent when $\frac{V \sin\alpha}{V_h} <$ -2 (windmill braking state):

$$\frac{v_i}{v_h} = -\frac{V \sin\alpha}{2v_h} - \sqrt{\frac{(V \sin\alpha)^2}{4v_h^2} - 1} \tag{32}$$

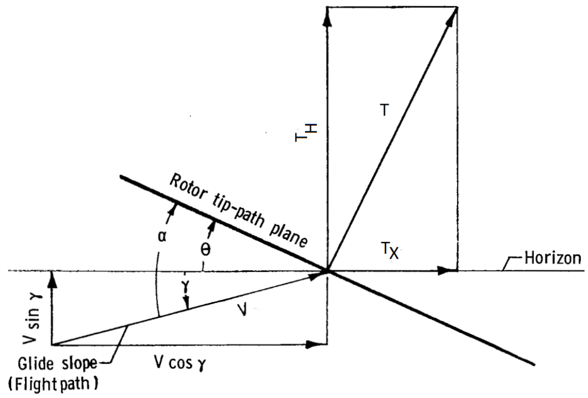

Figure 4. Force and velocity vectors during autorotation[20]

IV. Numerical Study

The equations of motion of the multi-rotor eVTOL vehicle (EHang 184) are continuous-time nonlinear differential equations which are difficult to solve analytically. For this reason, the vertical trajectory optimization problems are numerically solved using a pseudospectral method. Pseudospectral methods transcribe a multiphase optimal control problem to a large sparse nonlinear programming problem (NLP).[26,27] We used GPOPS-II[26,27] for transcribing the eVTOL's optimal control problems to the corresponding NLPs using hp-adaptive Gaussian quadrature collocation, these NLPs were then solved using IPOPT.[26,27,30]

As EHang 184 is a short range and slow speed eVTOL vehicle,[3] the starting point for the fixed final time arrival trajectory optimization problem has been chosen as 20 km along-track distance from the vertiport. For the case study 1 and 2, the initial condition (IC) and final condition (FC) for the multiphase optimal control problems are as shown in Table 1. Since the initial altitude and final altitude of the eVTOL vehicle are greater than $2Radius_{rotor}$ the in-ground effect (IGE) is neglected.[21]

Table 1. Initial and Final Conditions

State Variable	IC	FC
Altitude (m)	500	5
Along-track distance (m)	0	20000
Time (s)	0	RTA (t_f)

The performance data of EHang 184 used for aerodynamics and momentum theory related computations are as shown in Table 2.

Table 2. Performance Data

Variable	Value
Rotor Diameter (m)	1.6
Mass (kg)	240
Equivalent Front Plate Area (m^2)	2.11
Equivalent Top Plate Area (m^2)	1.47

A. Case Study 1: Energy Efficient Vertical Trajectories of the Fixed Pitch eVTOL Vehicle

In this case study, the energy efficient trajectories were generated by assuming EHang 184 as a fixed pitch eVTOL vehicle. Further, the pitch angle of the fuselage of the eVTOL vehicle is assumed to be same as the pitch angle of the tip-path-plane of the rotors ($-6° \leq \theta_{rotor} \leq 6°$). Figure 5, shows that for the energy efficient trajectories, the delay, i.e., increase in RTA (21, 23, 25, 28 and 30 minutes) is progressively absorbed by shortening of the cruise segment followed by flying a shallower descent (i.e. TOD is computed further away from the destination). From Figure 5 and Figure 6, it can also be inferred that the lower and upper control bounds of +/- 6 degrees on the rotor pitch angle are insufficient to fly at 27.7778 m/s, i.e., cruise speed of EHang 184. The sharp increase or decrease in control variables during the vertical phase transition can be attributed to the problem formulation assumption of quasi-steady flight with point mass model for the eVTOL vehicle and numerical error due to using less accurate numerical method, i.e. direct method to solve the multiphase optimal control problem.

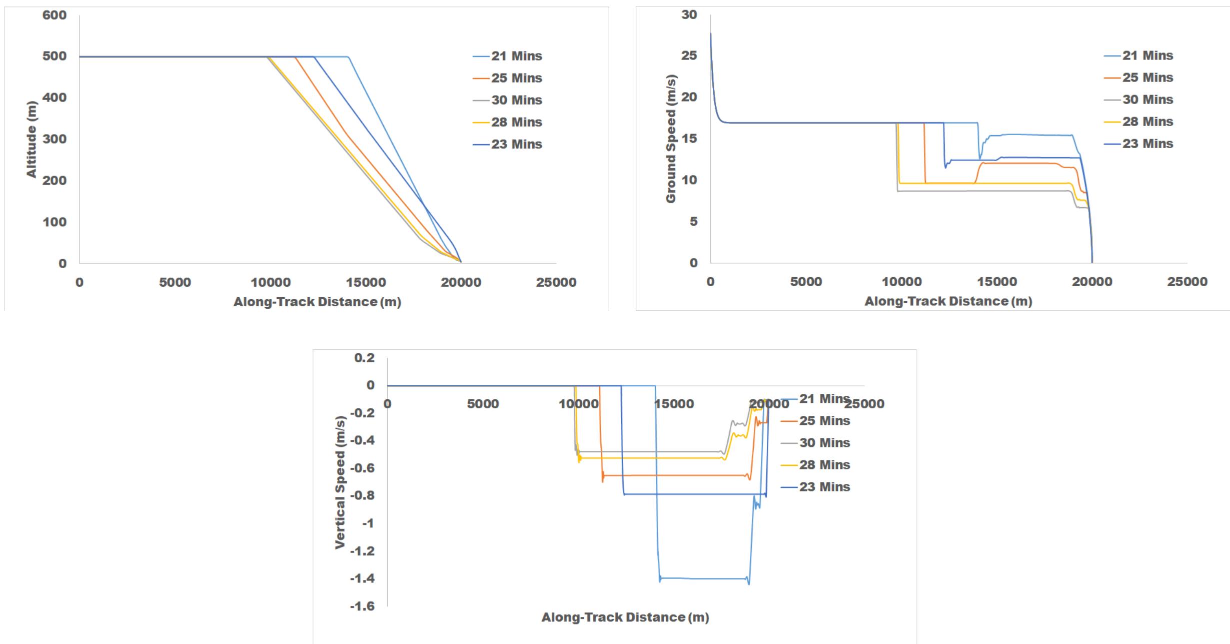

Figure 5. Energy efficient altitude, ground speed and vertical speed profiles of the fixed pitch eVTOL vehicle under various RTAs

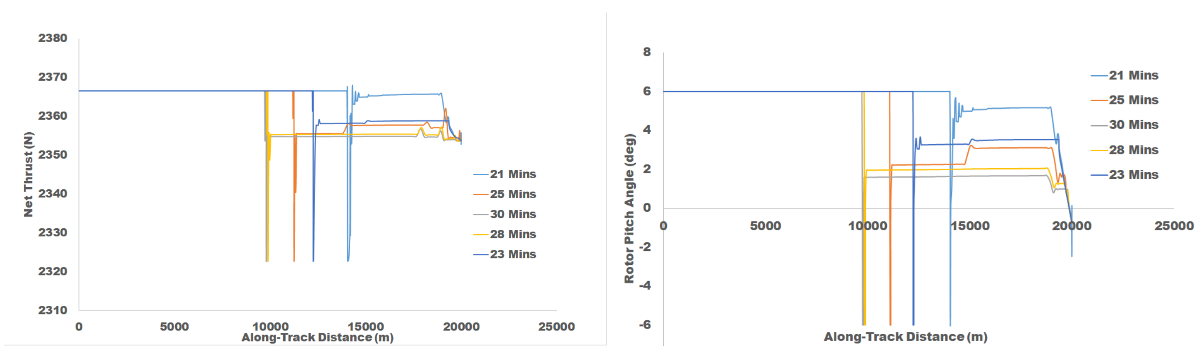

Figure 6. Energy efficient control strategy of the fixed pitch eVTOL vehicle under various RTAs

B. Case Study 2: Energy Efficient Vertical Trajectories of the Collective Pitch eVTOL Vehicle

The results of this case study were generated without imposing control bounds on the pitch angle of the tip-path-plane of the rotors, and the eVTOL vehicle is assumed to have a collective pitch mechanism. Figure 7 and Figure 8, shows that for the energy efficient trajectories, like in case study 1, the delay is absorbed by shortening of the cruise segment followed by flying a shallower descent (i.e. TOD is computed further away from the destination). However, unlike the case study 1, the optimal ground speed for the cruise segment is computed as 27.7778 m/s, i.e., EHang 184's cruise speed. As stated before, the sharp increase or decrease in control variables during the vertical phase transition can be attributed to the problem formulation assumption of quasi-steady flight with point mass model for the eVTOL vehicle and numerical error due to using less accurate numerical method, i.e. direct method to solve the multiphase optimal control problem.

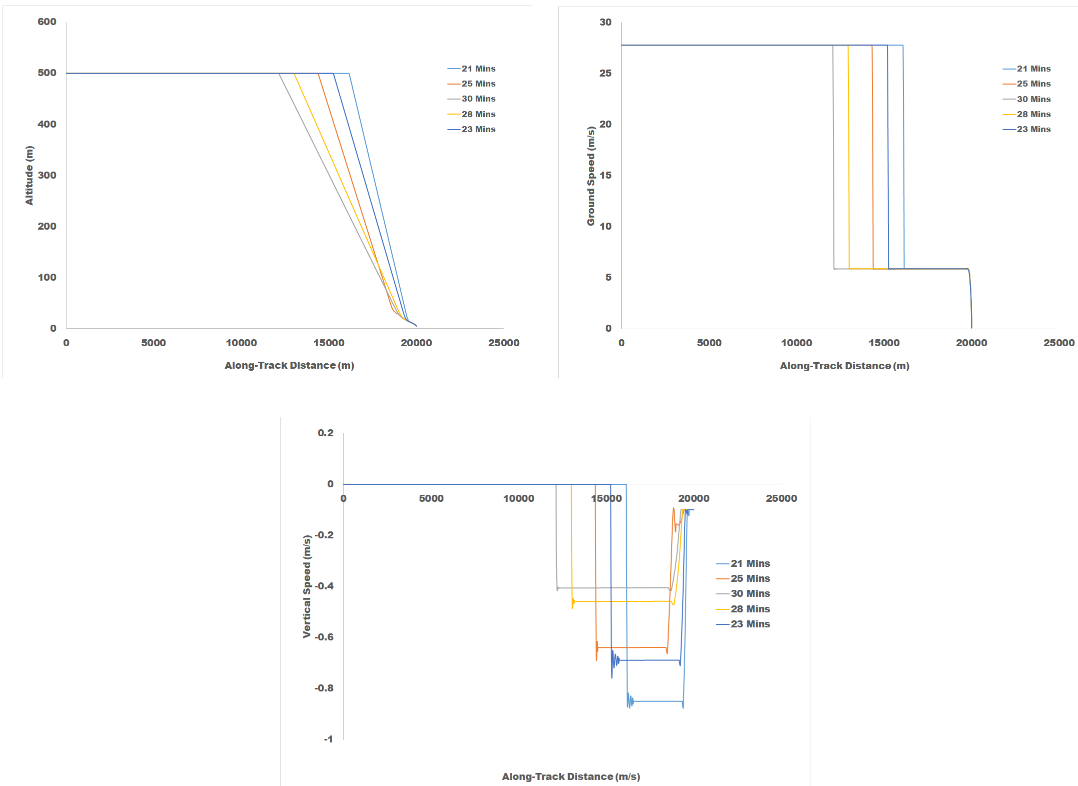

Figure 7. Energy efficient altitude, ground speed and vertical speed profiles of the collective pitch eVTOL vehicle under various RTAs

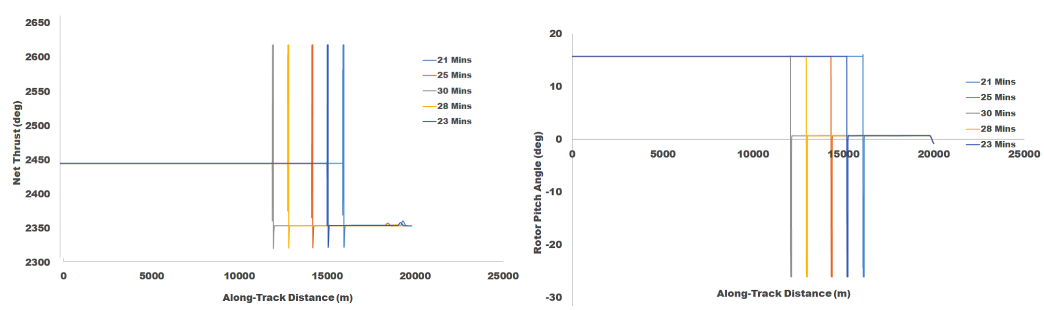

Figure 8. Energy efficient control strategy of the collective pitch eVTOL vehicle under various RTAs

C. Case Study 3: Effect of Cruise Altitude on Efficiency

The energy consumption results of the eVTOL vehicle at various cruise altitudes were computed by integrating the instantaneous power required for 20 minutes flight duration in cruise phase. As shown in Figure 9, the energy consumption of the eVTOL vehicle increases with increase in the cruise altitude for the same set of conditions (cruise speed, flight duration, and mass). The energy consumption results have the induced power loss as the dominant contributor of the two (induced and parasite) at the cruise speed of EHang 184. However, we anticipate in future with the possible increase in the operational cruise speed of a multirotor eVTOL vehicle like EHang 184, the cruise efficiency will improve with increase in the cruise altitude because of the reduction in the parasite drag (dominant contributor to the power loss at high speed) with increase in the altitude.

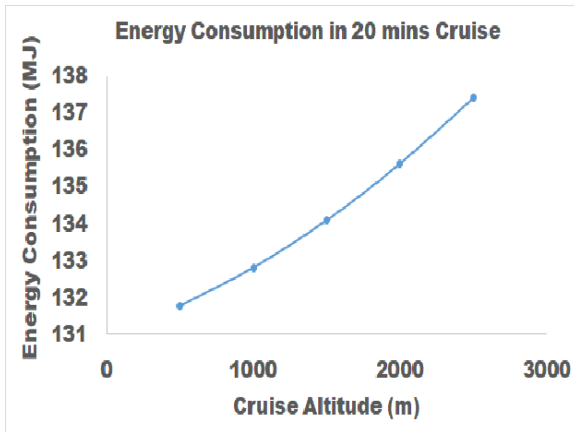

Figure 9. Energy consumption vs cruise altitude for the eVTOL vehicle

V. Conclusions

In this research, multiphase optimal control problem with energy consumption as the performance index is formulated for a multirotor eVTOL vehicle on an urban air mobility (UAM) passenger transport mission. Further, we present a framework to perform energy efficient arrival for a multirotor urban eVTOL air taxi given the required time of arrival (RTA) constraint. However, this proposed framework can also be used to address an energy efficient cargo delivery case in a UAS traffic management (UTM) context.

The formulated vertical trajectory optimization problem was numerically solved using pseudospectral method for a specific eVTOL vehicle, i.e., EHang 184. The numerical results of the fixed pitch case study suggest that the collective pitch mechanism is required for the operational feasibility of a multirotor eVTOL vehicle like EHang 184 considering passenger comfortness. Further, by imposing various arrival time constraints on the eVTOL vehicle, we found that for the energy efficient arrival operations, delay is best absorbed by shortening of the cruise segment followed by flying a shallower descent (i.e. TOD is computed further away from the destination). Also, the energy consumption case study shows that the cruise efficiency of EHang 184 drops with the increase in the cruise altitude. The energy consumption results also show that the induced power loss is the dominant contributor of the two (induced and parasite) at the cruise speed of EHang 184. We anticipate in future with the possible increase in the operational cruise speed of a multirotor eVTOL vehicle like EHang 184, the cruise efficiency will improve with increase in the cruise altitude because of the reduction in the parasite drag (dominant contributor to the power loss at high speed) with an increase in the altitude.

VI. Future Work

In our future work, we will consider the following: (i) vertical trajectory optimization of a multirotor eVTOL air taxi under wind impact; (ii) trajectory optimization of a tandem tilt-wing eVTOL; (iii) arrival scheduling of multiple eVTOL air taxis.

VII. Acknowledgment

The authors would like to specially thank Hokkwan Ng and Gilbert Wu at NASA Ames Research Center for their technical reviews and valuable recommendations. We would also like to thank Eric Mueller and Parimal Kopardekar at NASA Ames Research Center, Karthik Balakrishnan at Airbus A^3, and Jon Petersen and Mark Moore at Uber Elevate for the inspiring and encouraging discussions.

References

[1]Schrank, D., Eisele, B., Lomax, T., and Bak, J., "2015 urban mobility scorecard," 2015.

[2]Hoehner, C. M., Barlow, C. E., Allen, P., and Schootman, M., "Commuting distance, cardiorespiratory fitness, and metabolic risk," *American journal of preventive medicine*, Vol. 42, No. 6, 2012, pp. 571–578.

[3]Uber-Elevate, "Fast-forwarding to the future of on-demand, urban air transportation," https://www.uber.com/, 2017, [Online; accessed 19-November-2017].

[4]Prevot, T., Rios, J., Kopardekar, P., Robinson III, J. E., Johnson, M., and Jung, J., "UAS traffic management (UTM) concept of operations to safely enable low altitude flight operations," *16th AIAA Aviation Technology, Integration, and Operations Conference*, 2016, p. 3292.

[5]Airbus-A^3, "Future of urban mobility," http://www.airbus.com/newsroom/news/en/2016/12/My-Kind-Of-Flyover.html/.

[6]Altawy, R. and Youssef, A. M., "Security, Privacy, and Safety Aspects of Civilian Drones: A Survey," *ACM Transactions on Cyber-Physical Systems*, Vol. 1, No. 2, 2016, pp. 7.

[7]Park, S. G. and Clarke, J.-P., "Vertical trajectory optimization for continuous descent arrival procedure," *AIAA Guidance, Navigation, and Control Conference*, 2012, p. 4757.

[8]Robinson III, J. E. and Kamgarpour, M., "Benefits of continuous descent operations in high-density terminal airspace under scheduling constraints," .

[9]Clarke, J.-P. B., Ho, N. T., Ren, L., Brown, J. A., Elmer, K. R., Tong, K.-O., and Wat, J. K., "Continuous descent approach: Design and flight test for Louisville International Airport," *Journal of Aircraft*, Vol. 41, No. 5, 2004, pp. 1054–1066.

[10]Pradeep, P. and Wei, P., "Predictability, variability and operational feasibility aspect of CDA," *Aerospace Conference, 2017 IEEE*, IEEE, 2017, pp. 1–14.

[11]Jin, L., Cao, Y., and Sun, D., "Investigation of potential fuel savings due to continuous-descent approach," *Journal of Aircraft*, Vol. 50, No. 3, 2013, pp. 807–816.

[12]Cao, Y., Kotegawa, T., and Post, J., "Evaluation of continuous descent approach as a standard terminal airspace operation," .

[13]Dalmau, R., Verhoeven, R., de Gelder, N., and Prats, X., "Performance comparison between TEMO and a typical FMS in presence of CTA and wind uncertainties," *2016 IEEE/AIAA 35th Digital Avionics Systems Conference (DASC)*, Sept 2016, pp. 1–8.

[14]Coppenbarger, R. A., Mead, R. W., and Sweet, D. N., "Field evaluation of the tailored arrivals concept for datalink-enabled continuous descent approach," *Journal of Aircraft*, Vol. 46, No. 4, 2009, pp. 1200.

[15]EHang-184, "EHANG 184 autonomous aerial vehicle specs," http://www.ehang.com/ehang184/specs/, 2017, [Online; accessed 06-June-2017].

[16]Hoffmann, G., Huang, H., Waslander, S., and Tomlin, C., "Quadrotor helicopter flight dynamics and control: Theory and experiment," *AIAA Guidance, Navigation and Control Conference and Exhibit*, 2007, p. 6461.

[17]Bottasso, C. L., Croce, A., Leonello, D., and Riviello, L., "Rotorcraft trajectory optimization with realizability considerations," *Journal of Aerospace Engineering*, Vol. 18, No. 3, 2005, pp. 146–155.

[18]Yomchinda, T., Horn, J., and Langelaan, J., "Flight path planning for descent-phase helicopter autorotation," *AIAA Guidance, Navigation, and Control Conference*, 2011, p. 6601.

[19]Johnson, W., "Helicopter optimal descent and landing after power loss," 1977.

[20]Heyson, H. H., "A momentum analysis of helicopters and autogyros in inclined descent, with comments on operational restrictions," 1975.

[21]Johnson, W., *Helicopter theory*, Courier Corporation, 2012.

[22]DeMoss, J. A., *Drag measurements on an ellipsoidal body*, Ph.D. thesis, Virginia Tech, 2007.

[23]Pradeep, P., Park, S. G., and Wei, P., "Trajectory Optimization of Multirotor Agricultural UAVs," *to appear in Aerospace Conference, 2018 IEEE*, IEEE, 2018, pp. 1–7.

[24]Leishman, J., *Principles of Helicopter Aerodynamics*, Cambridge Aerospace Series, Cambridge University Press, 2002.

[25]Morbidi, F., Cano, R., and Lara, D., "Minimum-energy path generation for a quadrotor UAV," *Robotics and Automation (ICRA), 2016 IEEE International Conference on*, IEEE, 2016, pp. 1492–1498.

[26]Rao, A. V., Benson, D. A., Darby, C., Patterson, M. A., Francolin, C., Sanders, I., and Huntington, G. T., "Algorithm 902: Gpops, a matlab software for solving multiple-phase optimal control problems using the gauss pseudospectral method," *ACM Transactions on Mathematical Software (TOMS)*, Vol. 37, No. 2, 2010, pp. 22.

[27]Garg, D., Patterson, M., Hager, W. W., Rao, A. V., Benson, D. A., and Huntington, G. T., "A unified framework for the numerical solution of optimal control problems using pseudospectral methods," *Automatica*, Vol. 46, No. 11, 2010, pp. 1843–1851.

[28]Chenglong, L., Zhou, F., Jiafang, W., and Xiang, Z., "A vortex-ring-state-avoiding descending control strategy for multi-rotor UAVs," *Control Conference (CCC), 2015 34th Chinese*, IEEE, 2015, pp. 4465–4471.

[29]Smedt, D. d., Bronsvoort, J., and McDonald, G., "Controlled time of arrival feasibility analysis," 2013.

[30]Wächter, A. and Biegler, L. T., "On the implementation of an interior-point filter line-search algorithm for large-scale nonlinear programming," *Mathematical programming*, Vol. 106, No. 1, 2006, pp. 25–57.